ADIBEAM: Design and Experimental Validation of a Robust Beamforming Platform for Galileo Reference Ground Stations

Joan Manuel Cebrian
Joan Picanyol
Communications and Navigation Applications
Indra Espacio S.A.
Barcelona, Spain
jmcebrian@indra.es

Laura Gonzalez
Cristina Lavin
Oscar Gago
TTI Santander
Santander, Spain
lgonzalez@ttinorte.es

Francisco Amarillo
TEC-ETN – ESA/ESTEC
European Space Agency
Noordwijk, The Netherlands
francisco.amarillo@esa.int

Gonzalo Seco-Granados
Jose Lopez Vicario
Marc Barceló
Marti Mañosas
SPCOMNAV
Universitat Autonoma de Barcelona
Cerdanyola, Spain
gonzalo.seco@uab.es

Felix Antreich
Nikola Basta
Manuel Cuntz
Marcos V.T.Heckler
Matteo Sgammini
Institute of Communications and Navigation
German Aerospace Center (DLR)
Oberpfaffenhofen, Germany
Felix.Antreich@dlr.de

Abstract—**the increase in navigation accuracy demanded by EGNOS and Galileo and their future evolution encourages the study and design of advance receiver architectures. In that direction, the ADIBEAM project focuses on the design of high accuracy ground stations, specifically GNSS Reference Stations, in order to improve its robustness in front of multipath and interference errors with the goal of achieving centimeter level tracking accuracy. The adoption of antenna arrays and digital beamforming at the ground reference station receivers is one of the most promising approaches to cope with errors induced by multipath and interference.**

This paper proposes an innovative design of a ground based tracking station. In particular, the architecture proposed is based on the use of an antenna array and digital beamforming techniques, considering both adaptive and deterministic methods. The work carried out here considers the ground based tracking system, including the characterization of the system components (antennas, RF chains, calibration techniques, GNSS software receiver and digital beamforming), and the development of a software based experimentation platform representative of the proposed design for a hardware prototype. The sensitivity to perturbations and the extreme difficulty to perfectly control and calibrate all the components of the system, especially regarding the antenna array implementation, requires that the proposed design take into consideration not only the benefits of the possible solutions but also their feasibility for a real implementation.

In summary, this paper will present the design proposed and the Experimentation Platform used for its validation.

Keyword : Adaptive Digital beamforming; Antenna array; Ground Station; Multipath mitigation; Interfrence Mitigation.

I. INTRODUCTION

ADIBEAM project is a study of the European Space Agency with the objective to define a Ground-Based Tracking System for L-Band GNSS signals, specifically Galileo Signals, that provides enhanced performance in terms of multipath rejection, interference rejection and gain in order to provide high accuracy measurements. Such design will take advantage of the multiple studies in the field of adaptive digital beamforming for GNSS receiver systems.

The main advantages of using antenna arrays for the reception of GNSS signals is the possibility to suppress interference and multipath by introducing nulls in the directions where these come from and simultaneously to point the main beam in the desired direction. This improves the signal-to-noise and the signal-to-interference ratios of the whole system.

This study targets a solution for professional GNSS tracking stations requiring cm and mm accuracy in terms of code and carrier tracking errors, respectively.

THE WORK REPORTED IN THIS ARTICLE HAS BEEN SUPPORTED UNDER A CONTRACT OF THE EUROPEAN SPACE AGENCY (ADIBEAM AO/1-5934/08/NL/AT). THE VIEWS PRESENTED IN THE PAPER REPRESENT SOLELY THE OPINION OF THE AUTHORS AND SHOULD BE CONSIDERED AS R&D RESULTS NOT NECESSARLILY IMPACTING THE EGNOS AND GALILEO SYSTEM DESIGN

The Ground-Based Tracked System is designed to obtain the Signal In Space observables and navigation data disseminated by the GPS and Galileo constellation. In such a Galileo ground reference station solution, the data should then transmitted to the Galileo Control Centre through the wide area network, to feed the Orbitography and Integrity Processing Facilities with the aim to provide the system with accurate satellite ephemeris and clock prediction models.

The GBTS prototype shall be capable of simultaneously processing GPS and Galileo constellations. However, within this project, the requirements have been focused on Galileo Safety-of-Life signals.

Specifically, in the context of Galileo Sensor Station improvement, GBTS would process the data from the 2 carrier frequencies (L1/E1 and L5/E5b) carrying the SoL Galileo services transmitted by each Galileo spacecraft. The final GBTS would support the Galileo and GPS constellation, being able to process the Signal In Space from the satellites in view above 5° elevation (configurable mask angle), up to a maximum of 16 satellites.

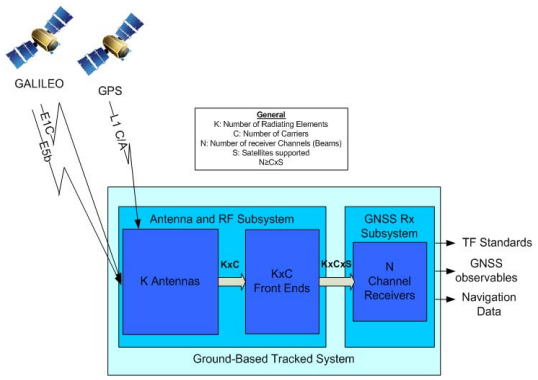

Figure 1: GBTS Context Diagram

The main problem arising when an antenna array is implemented in practice is the extreme difficult to perfectly control and calibrate all the components of the system. Typical array perturbations are due to the non –ideal response of the hardware elements (antenna and RF chains), mutual coupling effects, cross-polarization coupling, antenna position errors, etc. Indeed, the array performance is quite sensitive to these perturbations, showing dramatic performance losses if these are not carefully addressed. For that reason, this paper gives special emphasis to these issues, addressing them:

1) Designing an antenna array based on a planar rectangular deployment of micro-strip elements. The motivation of such option comes from the fact that this is feasible and ready-to-use solution for practical implantation thanks to the reproducibility of antenna conditions, ease of calibration and manufacturing, etc.

2) Introducing an online (and real-time) calibration mechanism aimed at compensating the spurious differences between the radiating elements and receiver channels from their nominal parameters. The proposed mechanism allows for the simultaneous operation of the GNSS receiver and the calibration (i.e. the calibration can be performed while the GNSS receiver is running and tracking satellite signals).

3) Proposing robust digital beamforming techniques able to cope with the residual perturbations and the particular difficulties associated with the signal scenario in ground stations (such as the presence of coherent reflections and the need to track satellites at low elevations).

In the final phase of the project, the design proposed will be validated by a representative Experimentation Platform in the section V. More specifically, this platform is based on the software simulation of all the GBTS components and Beamforming algorithms integrated in a GNSS software receiver block.

II. DESIGN PROPOSED

A. Antenna and Array structure

The developed micro-strip technology contributes to the design of compact antenna arrays. It allows for efficient integration of antenna elements together with the feeding and matching circuitry. A dual-patch technique (Figure 2:) for broadening the operation band was required for reception in E5 and E1. Quadruple sequential feeding was implemented for good axial ratio performance (Figure II-2).

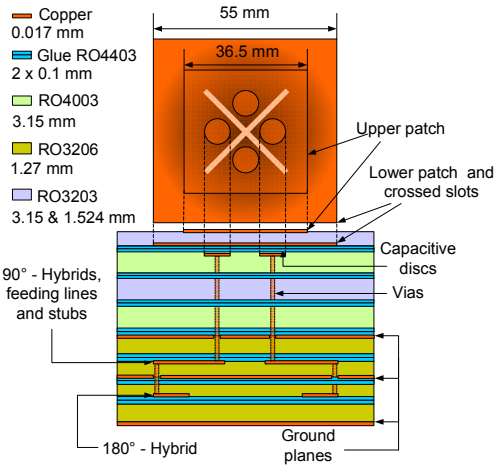

Figure 2: Single element architecture

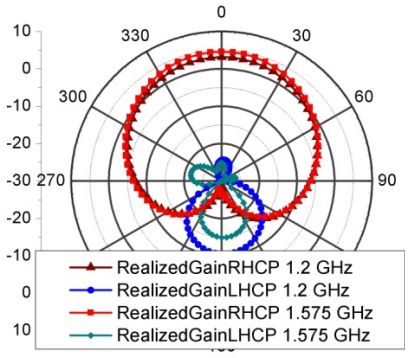

Figure 3: Radiation pattern (cut phi=0°)

Further on, adequate materials with sufficiently high electrical permittivity are used to reduce the antenna size to 95 mm × 95 mm in order to satisfy the inter-element distance condition regarding the grating lobes.

The designed antenna system is a 2-dimensional array of 6x6 elements in a rectangular structure. The distance between elements in x-axis and y-axis is 95mm.

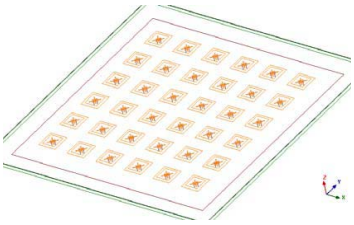

Figure 4: Layout of the 6x6 antenna array

Next figures show the radiation pattern of the 6x6 antenna array in the cut Phi=0º at 1.575 GHz using a deterministic beamformer that calculates the theoretical amplitude and phase excitation of each antenna element

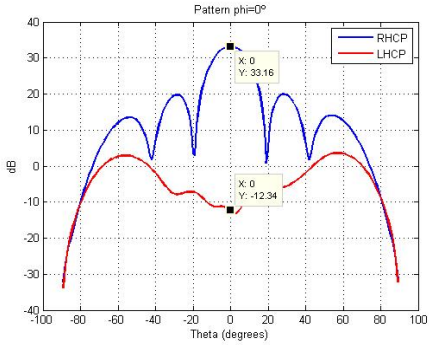

Figure 5: ERHCP and ELHCP for Psx=0º Psy=0º at 1.575GHz. Cut phi=0º. Thetagainmax= 0º

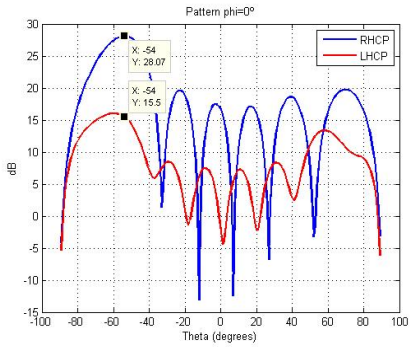

Figure 6: ERHCP and ELHCP for Psx=160º Psy=0º at 1.575GHz. Cut phi=0º. Thetagainmax=-54º

B. On-line Calibration

In a practical system, one of the main difficulties in an antenna array is to calibrate the amplitude and phase of every channel over temperature and frequency. In order to allow performing calibration without the need of removing the antenna array to an anechoic chamber, it is intended to integrate a calibration network in the antenna structure using strip-line technology. This network should distribute the calibration signal to each individual array element to enable the calibration of each channel starting from the output of the stacked patches up to the output of the front-end.

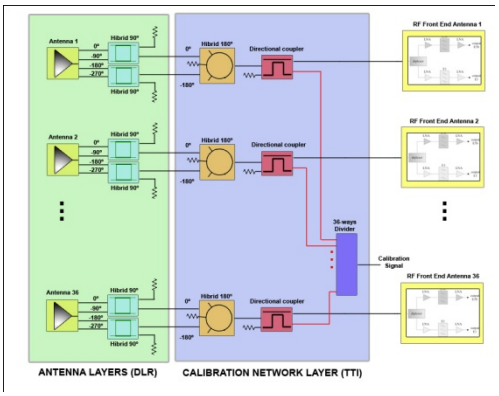

Figure 7: Block diagram of the antenna system and the calibration network

36 directional couplers are used to prevent calibration signal from being transmitted to each antenna port. The simulated specifications of the directional couplers are summarized in the following table:

Table 1 Specifications of the simulated directional coupler

Directional coupler specifications		
	1.200GHz	**1.575GHz**
Input matching	-29.33dB	-40.98dB
Insertion losses	-0.16dB	-0.178dB
Coupling factor	-21.34dB	-22.54dB
Isolation	-48.76dB	-57.36dB

To distribute this signal to the whole antenna system, a power splitter has been designed. The objective of this splitter is to achieve a good power distribution keeping the same phases between the 36 outputs corresponding to the 36 antenna-RF chains. The lengths of all the ways should be identical between them to achieve the same phase in the 36 outputs.

The following figures show the phase and power behaviours of the coupled ports (RF-chain port). It should be noted that the complete calibration network has been analysed (power divider and couplers).

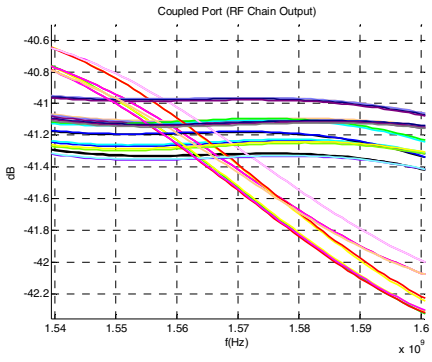

Figure 8: Power behaviour of the calibration network (coupled port) at 1.575GHz band

The power and the phase of all RF ports are very similar between them. The phases keep a difference of 11.1º in the worst case and the power has balance behaviour in all the ports

due to the fact that the most difference between ports is only 1.4dB. The ideal calibration network for 36 coupled outputs should be -38dB taking into account the directional coupler influences and considering an ideal distribution without insertion losses in the ways. The value shows in the graph show similar characterises to the ideal case.

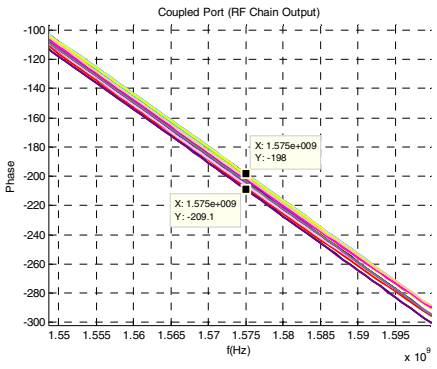

Figure 9: Phase behaviour of the calibration network (coupled port) at 1.575GHz band

Regarding the isolated port, the power signal at the Antenna system port is practically negligible. Consequently the calibration network provides a good behaviour due to the fact that the calibration signal is completely derived to the RF port, isolating the antenna system. The power behaviour at the antenna system port is depicted in **Error! Reference source not found.**. The graph demonstrates that the antenna ports are completed isolated because the power value is extremely low in all the cases.

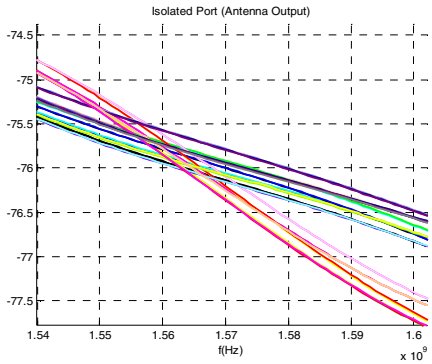

Figure 10: Power behaviour of the calibration network (isolated port) at 1.575GHz band

C. RF chains and ADC

The receiver shall acquire and track L1 and E5b signals from the Galileo satellites associated with SoL as described in Galileo ICD. For that reason the passive antenna of the receiving system is directly connected to an RF-board which contains a Diplexer to separate the E1 and E5b bands. One LNA for each band and a first band-pass filter for out of band interference suppression are used as an initial signal conditioning. **Figure 11** shows a schematic of the active antenna part, which is needed for each single antenna element.

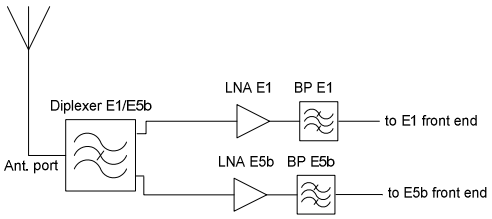

Figure 11: Active Antenna

Subsequently the amplified and filtered RF signals are fed to the frontend boards. The front ends for further amplification and down conversion are physically separated from the antenna array.

Because of the stated problems of the low IF and the direct RF sampling architectures, a conventional superheterodyne architecture for bandpass sampling is proposed in this project. With a maximum information bandwidth of 20 MHz, a theoretical sampling frequency of 40 MHz is sufficient. In addition, the conventional low IF super-heterodyne architecture is state of the art and can be well described by existing models. The incoming signal is first amplified in two stages and enters subsequently the mixing stage. The RF signal is mixed down to a low intermediate frequency. A low-pass filter eliminates the RF and LO breakthrough signals of the mixer. The signal is then amplified again by two stages and filtered by a band-pass anti aliasing filter. This band-pass filter allows subsampling the IF signal and thus reduce the sampling rate. Before the signal enters the ADC it passes a variable gain amplifier to adjust the right power level. The ADC uses 14 bits to sample the IF signal. These results in an effective dynamic range of over 65 dB which is suficient to transfer the received signal containing interference to the digital domain without loss of information. The figure below shows a block diagram of the front end architecture.

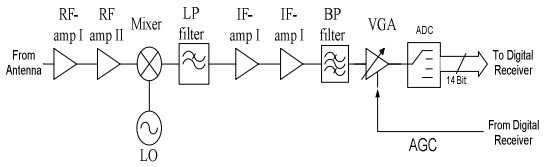

Figure 12: Front End Block diagram with band-pass sampling

D. GNSS Receiver

The proposed GNSS receiver architecture is presented in **Figure 13:**and can be summarized as follows:

- Tight integration with the beamformer where:
  a. Code correlators are placed before the beamfoming module (with the same frequency correction and time reference for all the antennas).
  b. Tracking loops are placed at the output of the beamforming module.
- Adoption of conventional acquisition and tracking blocks. As for the tracking blocks, the following DLL and PLL blocks are considered:

a. DLL with E-L spacing equal to 0.1 chips and bandwidth equal to 0.2 Hz.

b. PLL with bandwidth equal to 3 Hz.

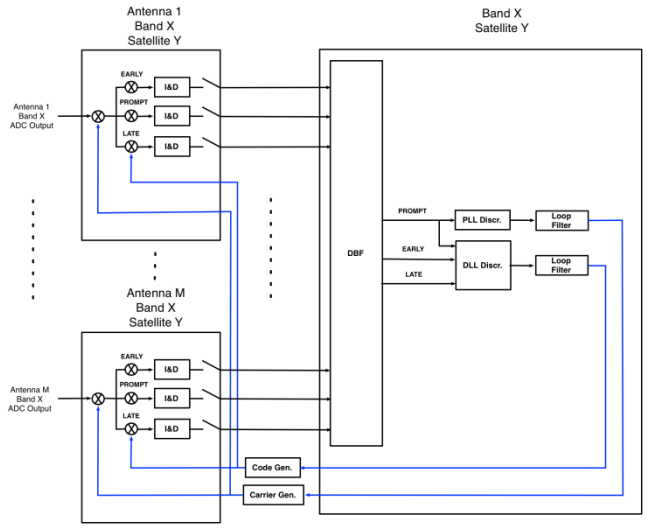

Figure 13: Receiver Architecture based on Antenna Array

The justification from such design solution is based on two premises:

- A tight integration with the beamformer is necessary in order to fully exploit the advantages of a multi-antenna receiver. That is to say, the beamformer and the receiver cannot be considered as independent units. Although this would have the benefit that a conventional receiver could be used, there would be serious performance limitations as only very simplistic pre-correlation beamformer would be possible.

- In spite of the tight integration, it is desired to build the receiver using the blocks usually found in conventional receivers, without changing their implementation, only their number and arrangement. The optimization of these blocks, such as the correlators and the tracking loops, has been carried out with great detail by the manufacturers. The fact that the design of such blocks need not be changed would pave the way for the adoption of antenna array technology by GNSS receiver manufacturers.

Concerning the parameters selected for the tracking loops, such selection is aimed at achieving low tracking errors. In other words, since the considered scenario is static, we focus the DLL design on the use of a solution oriented to the noise reduction in order to minimize tracking errors as much as possible. Concerning the PLL, we use the optimal arctangent solution because the reference stations are not complexity limited. Concerning the PLL bandwidth selection, the choice is aimed at alleviating scintillation effects. As reflected in some papers addressing ionosphere scintillation effects [5], the considered PLL bandwidth usually takes values between 1 and 10 Hz. In this work, we consider a value of 3 Hz in order to attain a good trade-off in terms of noise reduction vs. tracking of the carrier phase scintillation.

III. DIGITAL BEAMFORMING ALGORITHMS

A. Introduction

As has been previously stated, post-correlation beamforming as described in the **Figure 13:** has been considered. For each satellite and signal Galileo band (Galileo E1 and E5b) one digital beamformer has to be implemented.

An overview of the information that is to be available for the weight control unit is given in the **Figure 14**.

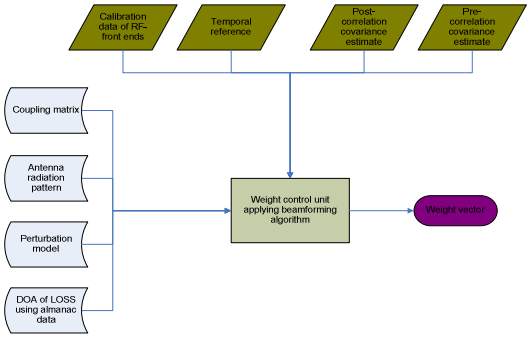

Figure 14: Available information to serve as input for weight control unit

In the following sections, we present the proposed digital beamforming algorithms. In particular, we first propose a deterministic beamfomer aimed at cancelling the entire interference and multipath region. Afterwards, we also consider one adaptive beamformer based on the IAA approach, showing a robust behaviour against coherent signals.

B. DET: Deterministic Beamformer

Among the set of deterministic approaches, the most popular designs are based on conventional beamformers pointing to the direction the interest and the application of spectral weighting in order to reduce the sidelobe level response (see [8] for further details). In this project, we compared different weighting schemes (uniform, discrete prolate spheroidal sequences, raised cosine, Kaiser, cosine weighting, Blackman-Harris and Dolph-Chebychev) and it was observed that the best performance was obtained with Dolph-Chebychev weighting. However, due to the particularities of the considered scenario (attenuation of the pattern should be assured in a specific region, i.e., elevations lower than 7.5º), we finally considered a deterministic approach that allows the design of desired pattern responses [9].

The design procedure of DET beamformer starts by defining the specification of the desired pattern. To do so, we define three parameters: the DOA of the LOSS signal (θ_d and φ_d), the sidelobe region of interest (Ω) and the desired response level at this region (ε). With this information in mind the algorithm is initialized as follows:

$$\min_{\mathbf{w}} \mathbf{w}^H \mathbf{A} \mathbf{w}$$
$$s.t.\ \ \mathbf{w}^H \mathbf{v}(\theta_d, \varphi_d) = 1$$

where $\mathbf{w}$ is the beamforming vector, $\mathbf{v}(\theta_d, \varphi_d)$ is the steering vector associated to the DOA of the LOSS [7] and

matrix $\mathbf{A} = \sum_{(\theta_i,\varphi_i)\in\Omega} \mathbf{v}(\theta_i,\varphi_i)\mathbf{v}^H(\theta_i,\varphi_i)$ simulates the covariance matrix of a scenario with a dense set of interference signals uniformly distributed in the sidelobe region (being in our case the region covered by $0 \le \theta \le 7.5^o$ and $0 \le \varphi \le 360^o$). In practice, this matrix is constructed by uniformly dividing the region of interest in T points. Nonetheless, we have observed in our experiments that good performance results can be obtained by selecting the identity matrix instead of matrix **A** and, by doing so, the complexity of the method is considerably reduced. It is worth noting that an additional constraint was included in the original algorithm [9] in order to assure that the maximum gain is obtained in the desired direction. However, our experiments revealed that this constraint is not needed in the considered planar array. Besides, performance is improved as two degrees of freedom are saved.

The initialization step is a constrained optimization problem with the objective of assuring a distortionless response for the desired signal and the minimization of all the directions coming from the sidelobe region Ω. Therefore, the solution can be easily obtained by means of the Lagrangian method as follows:

$$\mathbf{w}^H = \frac{\mathbf{v}^H(\theta_d,\varphi_d)\mathbf{A}^{-1}}{\mathbf{v}^H(\theta_d,\varphi_d)\mathbf{A}^{-1}\mathbf{v}(\theta_d,\varphi_d)}$$

However, a response level equal to ε is not assured in the sidelobe region. For that reason, additional iterations are included in the algorithm in order to attain the desired response. More specifically, the beamformer is updated at each iteration as follows:

$$\mathbf{w} = \mathbf{w} + \Delta\mathbf{w}$$

where $\Delta\mathbf{w}$ is the solution to the following problem:

$$\begin{aligned} &\min_{\mathbf{w}} \Delta\mathbf{w}^H\mathbf{A}\Delta\mathbf{w} \\ &s.t.\ \ \Delta\mathbf{w}^H\mathbf{v}(\theta_d,\varphi_d) = 0 \\ &\qquad \Delta\mathbf{w}^H\mathbf{v}(\theta_j,\varphi_j) = f_j \qquad \text{for } j = 1..M-1 \end{aligned}$$

The above constraints are imposed to assure that the distortionless property is maintained ($(\mathbf{w}+\Delta\mathbf{w})^H\mathbf{v}(\theta_d,\varphi_d) = 1$ if $\Delta\mathbf{w}^H\mathbf{v}(\theta_d,\varphi_d) = 0$) and that the directions in the region Ω with the highest response ($(\theta_j,\varphi_j) = f_j,\ j = 1..M-1$) attain the desired response (f_j is computed as $f_j = (\varepsilon - |c_j|)c_j / |c_j|$, being c_j the response to the previous beamformer $\mathbf{w}^H\mathbf{v}(\theta_j,\varphi_j) = c_j$). By defining matrix

$$\mathbf{C} = \left[\mathbf{v}(\theta_d,\varphi_d), \mathbf{v}(\theta_1,\varphi_1), ..., \mathbf{v}(\theta_{M-1},\varphi_{M-1})\right]$$

and vector $\mathbf{g} = \left[0, f_1, ..., f_{M-1}\right]^T$, the following solution is obtained for $\Delta\mathbf{w}$:

$$\Delta\mathbf{w}^H = \mathbf{g}^H\left(\mathbf{C}^H\mathbf{A}^{-1}\mathbf{C}\right)^{-1}\mathbf{C}^H\mathbf{A}^{-1}$$

With the obtained result, the beamforming vector is updated and the algorithm is iterated until convergence. In situations where convergence is attained, the number of required iterations depends on the target pattern response but it is usually of the order of the number of antennas.

It is worth recalling that this is a deterministic beamformer. Thus, the beamforming solution for the different LOSS DOAs can be computed off-line and saved.

C. IAA: Iterative Adaptive Algorithm

The Iterative Adaptive Approach (IAA) method is an adaptive beamformer based on a robust design criterion. This algorithm was selected due to its good behavior in terms of robustness as reported in [3]. More specifically, the authors in [3] compared the IAA beamformer with other robust approaches and showed that this option is the most equilibrated strategy in terms of SINR, DOA estimation accuracy and desired signal power.

Further details of the algorithm can be found in [6] but basically the idea consists in defining a scanning grid of L directions by constructing a set of L steering vectors $\mathbf{V} = \left[\mathbf{v}_1, ..., \mathbf{v}_L\right]$. Once this scanning grid is defined, the algorithm estimates the powers at each direction and gathers them in matrix $\hat{\mathbf{P}} = diag(\hat{P}_1, ..., \hat{P}_L)$. After that, the beamformer for each direction (with a potential source) is computed as:

$$\mathbf{w}_l{}^H = \frac{\mathbf{v}_l{}^H\overline{\mathbf{R}}_x{}^{-1}}{\mathbf{v}_l{}^H\overline{\mathbf{R}}_x{}^{-1}\mathbf{v}_l}$$

where $\overline{\mathbf{R}}_x$ is a estimate of the covariance matrix iteratively computed by considering the received signal $\mathbf{x}(n)$ at the input of the digital beamforming block for N snapshots as follows:

$$\hat{s}_l(n) = \mathbf{v}_l{}^H\mathbf{x}(n)/M \qquad n = 1,...,N; l = 1,...,L$$

$$\hat{P}_l = \frac{1}{N}\sum_{n=1}^{N}|\hat{s}_l(n)|^2 \qquad l = 1,...,L$$

repeat

$\overline{\mathbf{R}}_x = \mathbf{V}\hat{\mathbf{P}}\mathbf{V}^H$

for $l = 1,...,L$

$\mathbf{w}_l^H = \dfrac{\mathbf{v}_l{}^H\overline{\mathbf{R}}_x{}^{-1}}{\mathbf{v}_l{}^H\overline{\mathbf{R}}_x{}^{-1}\mathbf{v}_l}$

$\hat{P}_l = \mathbf{w}_l^H\hat{\mathbf{R}}_x{}^{-1}\mathbf{w}_l$

end for

until convergence

where M is the number of antennas and $\hat{\mathbf{R}}_x$ is the sample covariance matrix of the received signal $\mathbf{x}(n)$. Notice that the beamforming solution is similar to the classical Capon approach and the robustness against array perturbations and coherent signals comes from two facts: 1) matrix $\hat{\mathbf{P}}$ is defined by considering that the sources are uncorrelated, and 2) the covariance matrix is estimated by taking into account the power arriving from the directions where the different beamformers are pointing, being this power estimate performed by taking into account the sample covariance matrix $\hat{\mathbf{R}}_x$

IV. EXPERIMENTATION PLATFORM IMPLEMENTATION

A. Experimentation Platform Overview

In the final phase of the project, the design proposed will be validated by a representative Experimentation Platform. More specifically, this platform is based on the software simulation of all the GBTS components (antennas and RF chains effects, etc.) and Beamforming algorithms integrated in a GNSS software receiver block. In addition, a RF Environment Simulator (RFES) block is necessary to test and validate the design proposed, since it generates the scenarios to be tested. Besides, with the aim to test the robustness of the proposed digital beamforming, different perturbation sources are introduced in the system (calibration errors, mutual coupling effects, etc.)

Next figure shows the different blocks that cover our Experimentation Platform:

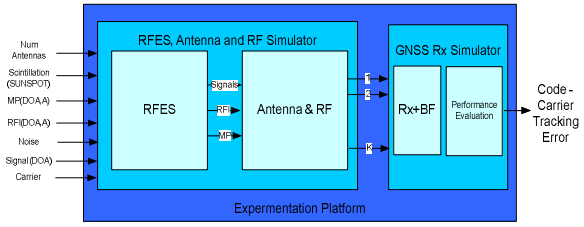

Figure 15: Context diagram

Both the RFES and the Antenna and RF Subsystem simulator are to be considered as closely related processing blocks which will be implemented together in one software block in order to simplify interfaces and implementation.

The input signals are first fed into the antenna transfer function block, which applies the direction-dependent amplitude-phase response of every array element to the input wavefronts. The amplitude and phase response characteristics of the array elements will account for several kinds of impairments, including inter-element electromagnetic coupling, polarization mismatch, radiation in the directions of the array edges, etc.

The array element outputs are then fed through the RF chain transfer function block, which simulates the effects (noise, amplitude and phase distortions, absolute group delay and its variation over frequency, etc.) introduced by the RF chain of each radiating element. A front end RF analysis will be performed in order to calculate its transfer function. Special emphasis will be put on modeling the interface between the radiating element and the first LNA stage in order to predict coupling losses.

The output data from the Antenna and RF Subsystem simulator will be used as input to the GNSS Receiver Subsystem simulator. The GNSS receiver and Beamforming algorithms will be implemented in another independent simulator.

B. Signal Generation

The Signal Generator emulates GNSS signals as they would appear in a real receiver after the receiver antenna and front-end. Simulated GNSS signals are E1 and E5b signals related to the SoL services. The signals are generated in a complex baseband band-limited representation [10].

Furthermore the generator takes in account several aspects related to the antenna and receiver chain like the antenna radiation pattern, considering both the cross-polar and co-polar components, antenna and array imperfections, antenna array mutual coupling, front-end filtering, ADC quantization, reference clock instability and AWGN.

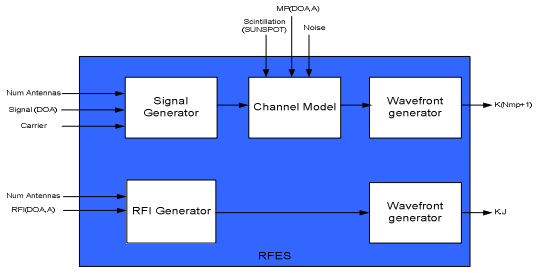

Figure 16: Radio frequency environment simulator

The software allows selecting different directions of arrival for the LOSS signal and for each of the multipath and interferers, the last are supposed to be ground-based and therefore an elevation lower than 7.5° has been considered.

Radio frequency interferers are also simulated and fed in the receiver chain without been affected by the propagation channel. Interferences are represented by a centred band-limited signal and generated using a raised-cosine function with a roll-off equal to 0.2 and a truncation factor equal to 24 which corresponds to a stop band attenuation of about 35dB.

The simulator implements different propagation channel effects affecting the GNSS signal like scintillation, Doppler variation and multipath.

Multipath amplitude and phase are aleatoric values following a gamma and uniform distribution respectively, the coherence time is a variable parameter and shall be greater than the receiver tracking loop bandwidth. Furthermore, in order to avoid sharply unrealistic variations, an interpolation process is performed acting as a smoothing function.

Scintillation simulation implements amplitude fading and phase variation based on a Nakagami-m and zero-mean Gaussian distribution respectively [14]:

$$E(t) = A(t) \cdot e^{i\phi} = A_0(t) \cdot \delta A(t) \cdot e^{i(\phi_0 + \delta\phi(t))}$$

Where δA and $\delta\phi$ are the intensity and the phase of the scintillation respectively.

The intensity of the scintillation is characterised by the S4 parameter:

$$S_4 = \frac{\sigma_{\delta I}}{E\langle \delta I \rangle}, \ where \ \ \delta I = \delta A^2$$

and $m = \frac{1}{S_4^2}$

Nakagami-m distribution is generated based on a trivariate gamma distribution [14]:

$$G_1(\alpha_1 - \rho\sqrt{\alpha_1\alpha_2}, \beta_1), \ G_2(\alpha_2 - \rho\sqrt{\alpha_1\alpha_2}, \beta_2) \ and \ G_3(\rho\sqrt{\alpha_1\alpha_2}, \beta_2)$$

where $\alpha_1 = 1/S_4^2$, $\beta_1 = S_4^2$, $\alpha_2 = \alpha_1/\rho^2$, $\beta_2 = 1$ and $\rho = 0.6$, ρ represents the correlation coefficient between the intensity and

the phase aleatoric values. The intensity and phase aleatoric values are then obtained combining the trivariate gamma distribution in a bivariate gamma distribution:

$X_I = G_1 + G_2$ $(Intensity)$, $X_\phi = G_2 - G_3$ $(Phase)$ and scaling $X_\phi \to N(0, \sigma_{\delta\phi})$ .Furthermore to generate more realistic power spectral densities the aleatoric vectors are filtered [12].

Scintillation parameter S4 and phase standard deviation $\sigma_{\delta\phi}$ are extrapolated using the Wideband Ionospheric Scintillation model (WBMOD) considering a sunspot number equal to 140, a receiver position close to the equatorial region, a Kp value of 4 and a receiver time starting from sunset to midnight [13].

GNSS signals are formed by a successively repetition of a reference band-limited pulse, which form depends on the channel modulation.

Output of the signal generator are binary files, one for each of the radiating element composing the antenna array. These files are used as input in the Software Receiver described in the next section.

C. *Software Receiver implementation*

Figure 17 shows the architecture of the Receiver subsystem simulator.

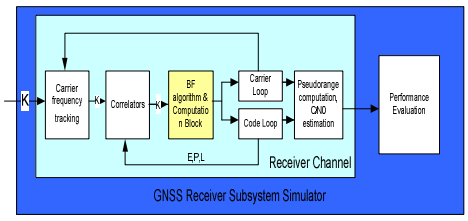

Figure 17: Adibeam Experimentation Platform: GNSS Receiver Subsystem Simulator

This subsystem receives the K signals processed by the Antenna and RF Subsystem (as would be received by K real radiating elements) and applies the digital beamforming and GNSS reception algorithms.

As a final step in the GNSS Receiver Subsystem, a performance evaluation block is included. In this block, statistics regarding code and carrier tracking error (bias and standard deviation) are obtained.

Like RFES simulator, this simulator has been implemented in MATLAB. Even though the simulator is not operating in real time, the implementation has been carefully designed so that the resulting tool is suitable and flexible enough for the experimentation.

More detail of the general architecture of the GNSS receiver and the implementation of the digital beamforming is depicted in the next figure.

By taking into account the results obtained during the design assessment, the pre-correlation option has been considered for the beamformer detailed design and Experimental Platform implementation. In this project we propose deterministic and adaptive beamforming algorithms implementation, and consequently the receiver has to be flexible enough to process both algorithms and receive different inputs.

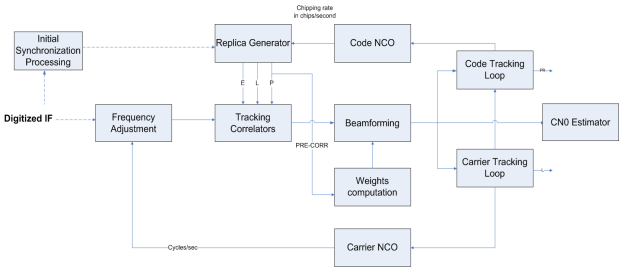

Figure 18: GNSS receiver general architecture

V. FUTURE WORK

A. *Future work*

In the final phase of the project, the design proposed will be validated by a representative Experimentation Platform. More specifically, this platform is based on the software simulation of all the GBTS components (antennas and RF chains effects, etc) and Beamforming altorithms integrated in a GNSS software receiver block described previously.

Besides, with the aim to test the robustness of the proposed digital beamforming, different perturbation sources are introduced in the system (caligration errors, mutual coupling effects, etc).

In future papers the results achieved through the Experimentation Platform used for the validation of the proposed design will be presented.

References

[1] F. Amarillo, A. Ballereau, M. Crisci, B. Lobert, and S. Lannelongue, "Galileo IOV ground mission segment performances," *in Proc. GNSSENC* 08

[2] K.A. Griffith and I.J. Gupta, "Effect of mutual coupling on the performance of gps aj antennas," *Navigation*, vol. 56, pp. 161–173, 2009.

[3] C.-L. Chang and J.-C. Juang, "A new pre-processing approach against array uncertainty for gnss," *Proc. Of IEEE/ION PLANS*, 2008.

[4] E. N. Lavado, M. V.T. Heckler, W. Elmarissi, and A. Dreher, "Dual-band microstrip antenna for a robust navigation receiver," *Proc. of ENCGNSS*, 09

[5] T. N. Morrissey, K. W. Shallberg, A. J. Van Dierendonck, and M. J. Nicholson, "GPS receiver performance characterization under realistic ionospheric phase scintillation environments," *Radio Science*, vol. 39, 2004.

[6] M. V. T. Heckler, W. Elmarissi, L. A. Greda, M. Cuntz, and A. Dreher, "Narrowband microstip antenna array for a robust receiver for navigation applications," *3rd European Conference of Antennas and Propagation*, 2009.

[7] D. H. Lee and C. S. Pyo, "Performance and effect of calibration in smart antenna system," *Radio Technology Research Group, ETRI (Electronics and Telecommunication Research Institute)*, 2004.

[8] H.L. Van Trees, *Optimum Array Processing (Detection,Estimation and Modulation Theory, Part IV)*, JohnWiley, 2002.

[9] C-Y. Tseng and L. J. Griffiths, "A simple algorithm to achieve desired patterns for arbitrary arrays," *IEEE Trans. on Signal Processing*, vol. 40, pp. 2737–2746, Nov. 1992.

[10] Winkel, J., Modeling and Simulating GNSS Signal Structures and Receivers, University of Federal Armed Forces Munich, 2003

[11] Nakagami, M., The m-distribution: A general formula of intensity distribution of rapid fading, in Statistical Mehods in Radio Wave Propagation, edited by W.C. Hoffman, pp.3-36, Pergamon, New York, 1960.

[12] Devroye, L., Non-uniform Random Variate Generation, pp.405, 407-410, 416-418 and 588, Springer-Verlag, New York, 1986

[13] Basu, S., E. MacKenzie, E. Costa, P. Fougere, H. Carlson and H. Whitney, 250 MHz/GHz scintillation parameters in the equatorial, polar and auroral environments, IEEE Selected Area Commun., SAC-5(2), 102-115